Nonreciprocal optical properties in resonant hybrid photonic crystals

A. D'Andrea and N. Tomassini
Istituto dei Sistemi Complessi, CNR, Cassella Postale 10, Monterotondo Stazione, I-00015 Rome, Italy
(Received 24 May 2016; published 22 July 2016)

The present work is devoted to the theoretical study of the nonreciprocal optical properties in hybrid (isotropic and anisotropic) periodic multilayers for photon energy values chosen close to the electronic energy gaps of semiconductors (excitons). The optical properties of these resonant nonmagnetic photonic crystals, where linear and quadratic spatial dispersion effects are both present, will be studied in the framework of exciton-polariton self-consistent solutions of the Maxwell and Schrödinger equations in the effective-mass approximation. The main interesting optical properties, namely, giant transmission, absorption suppression, and optical unidirectional propagation, will be computed by implementing a two-layer "minimum model."

DOI: 10.1103/PhysRevA.94.013840

I. INTRODUCTION

In the recent literature [1–6] many new optical effects in hybrid (isotropic-anisotropic) photonic crystals have been discussed. Among these, negative refraction, oblique frozen modes [2], giant transmission [3], absorption suppression [5], and optical unidirectional propagation [6] are among the most interesting ones. All these properties are studied from the theoretical analysis of the dispersion curves in these hybrid periodic multilayers, and the symmetry conditions, necessary to observe the former optical effects, are fully discussed [2–6].

Recently, the exciton-polariton, a composite particle coming from strong radiation-matter coupling, in photonic crystal resonators has demonstrated a wide range of spectacular new phenomena, such as optical spin-hole effects [7], magnetic dipole enhancement [8], Bose-Einstein condensation at room temperature [9,10], and radiative topological states [11].

Two different photonic resonators are usually used for confining exciton-polaritons in an optical cavity, namely, a microcavity with distributed Bragg reflectors [12] and the resonant quantum well Bragg reflectors [13]. While the former resonator is based on a photonic impurity of a dielectric periodic crystal in resonance with an exciton energy transition, the latter one is a periodic resonant exciton-polariton crystal [13]. Recently, we extended the optical response of the latter system to the resonant hybrid photonic crystals [14] where the exciton-polariton is in resonance with the lowest band-gap energy of a hybrid one-dimensional (1D) periodic multilayer for studying the possibility of stopping, storing, and releasing a light impulse [15] in periodic stacks of semiconductors.

In the present work, starting from a simple 1D symmetric hybrid resonant photonic crystal, by a continuum variation of the optical axis orientation of uniaxial layers, we will show as building up a nonreciprocal metamaterial where unidirectional propagation [2] can be observed.

It is widely accepted that in a two-dimensional (2D) photonic band of metamaterials with broken spatial inversion and time-reversal symmetries (nonreciprocal media), in the correspondence of a pair of Dirac points, the two bands split apart, and a nontrivial topology could be present [16]. In the present work a situation similar to the former one but based on an axial asymmetric dispersion relation [2] will be discussed, but the problem of under which conditions a nontrivial topology can be obtained is outside the scope of the present work.

Let us recall that, in a 1D periodic multilayer, the interference between different linear polarizations allows us to observe an absolute gap inside the Brillouin zone (BZ) [1,14]. In fact, while the forward and backward waves, with the same polarization, interfere constructively at the high-symmetry points of the BZ (Γ and $k = \pm\pi/d$), the interference between different polarized components can drop inside the BZ, giving a strong deformation of the photon density of states, and large rearrangements of the band gaps can be observed. In this case the density of state is proportional to k^4, where k is the Bloch wave vector [2], and for oblique incidence and energies close to the exciton-photon interaction, the former behavior is complemented by the center-of-mass density of states of the 2D Wannier exciton [13]. Finally, let us underline that the negative refraction propagation in uniaxial 1D multilayers is essentially due to the former behavior of the dispersion curves, as previously discussed in Refs. [1,14].

II. HYBRID RESONANT PHOTONIC CRYSTAL: THE MODEL

In the present work, a theoretical study of nonreciprocal optical properties in a periodic hybrid (isotropic-anisotropic) stack, where the anisotropic bilayer is composed of two uniaxial layers with different orientations of the optical $\hat{C}$ axis, is computed in the exciton-polariton framework [17] by self-consistent solutions of the Maxwell and Schrödinger equations in the effective-mass approximation for photon energies close to the electronic valence-conduction energy gap of the semiconductors (excitons). The cluster embodies N elementary cells and two surface quantum wells. Moreover, in order to avoid the Fabry-Pérot oscillations, due to the rather large number of layers of the cluster, antireflection is added on both surfaces of the stack.

Let us underline that the elementary cell of our "minimum model" (see Fig. 1) is composed of $\lambda/4$ uniaxial bilayers, with misalignment of the optical axes, and an isotropic $\lambda/4$ layer that embodies the optically active zone (quantum well) where a direct electron valence-conduction band transition is modeled by a Wannier exciton confined between two rather high isotropic barriers [14]. Since the optical properties of the system come from the structural properties of the sample

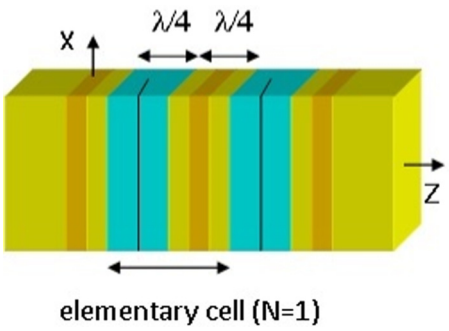

FIG. 1. One-dimensional hybrid (isotropic-anisotropic) multilayer. Brown layers are the quantum wells, yellow layers are the barriers of the quantum wells, and sky blue layers are the uniaxial layers.

and from the optical character of the incident light, in the present calculation we have embodied the maximum of optical information on the sample structure [14]. Moreover, in order to make clear the optical tailoring of the sample, in our minimum model each layer must control only a single optical parameter; therefore, we have adopted two uniaxial layers in the elementary cell, with the two optical axes making an angle α_L with respect to the x axis on the plane (x,y) on the left and an angle α_R with respect to the same x axis but this time lying on the plane (x,z), instead of a single uniaxial layer with a general optical axis orientation [2]. Therefore, the dielectric tensors of the left and right uniaxial layers are

$$\varepsilon_L = \begin{pmatrix} \varepsilon_\perp + \cos^2\alpha_L \Delta\varepsilon & \cos\alpha_L \sin\alpha_L \Delta\varepsilon & 0 \\ \cos\alpha_L \sin\alpha_L \Delta\varepsilon & \varepsilon_\perp + \sin^2\alpha_L \Delta\varepsilon & 0 \\ 0 & 0 & \varepsilon_\perp \end{pmatrix}, \quad (1a)$$

$$\varepsilon_R = \begin{pmatrix} \varepsilon_\perp + \cos^2\alpha_R \Delta\varepsilon & 0 & \cos\alpha_R \sin\alpha_R \Delta\varepsilon \\ 0 & \varepsilon_\perp & 0 \\ \cos\alpha_R \sin\alpha_R \Delta\varepsilon & 0 & \varepsilon_\perp + \sin^2\alpha_R \Delta\varepsilon \end{pmatrix}, \quad (1b)$$

where $\Delta\varepsilon = \varepsilon_\parallel - \varepsilon_\perp$ is the birefringence. The parameter values of the model are chosen along the lines of Ref. [14]; namely, let us take the background dielectric constant value of the semiconductors (well) as $\varepsilon_b = 10.24$ and, for a symmetric choice of parallel and orthogonal dielectric constants, $\bar{\varepsilon} = (\varepsilon_\parallel + \varepsilon_\perp)/2 = \varepsilon_b$. For not very large birefringence values $(\Delta\varepsilon = \varepsilon_\parallel - \varepsilon_\perp = 4)$, the two conditions give parallel and orthogonal dielectric constant values: $\varepsilon_\parallel = 12.24$ and $\varepsilon_\perp = 8.24$, respectively. The exciton transition energy for a direct valence-conduction parabolic band model is given by

$$E_{\rm ex}(\mathbf{K}_\parallel) = E_{\rm ex}(\mathbf{K}_\parallel = 0) + \frac{\hbar^2}{2M} K_\parallel^2, \quad (2)$$

where $\mathbf{K}_\parallel$ is the in-plane wave vector of the exciton center of mass (the total mass is $M = 0.524 m_o$), and the valence-conduction Kane's energy of the transition [17,18] is $E_K = 23$ eV, in sound agreement with AlGaAs/GaAs(001) systems. The exciton transition energy value $E_{\rm ex}(\mathbf{K}_\parallel = 0)$ and its corresponding envelope function are obtained with a variational solution of the Schrödinger equation in the effective-mass approximation [17,18].

For a so-called high-quality quantum well of thickness $L_w = 10$ nm a reasonable nonradiative broadening value [18] is $\Gamma_{NR} = 0.25$ meV, and exciton energy is $E_{\rm ex}(0) = 1.418$ eV; therefore, the resonant thickness is given by $\lambda/2 = \pi\, c/E_{\rm ex}(0)\sqrt{\varepsilon_b}$. Finally, in order to preserve strong radiation-matter interaction and an unperturbed Wannier exciton envelope function, in the otherwise asymmetric elementary cells, some added conditions are adopted, as fully discussed in Ref. [14].

III. SPATIALLY ASYMMETRIC ELEMENTARY CELL

Now, let us briefly summarize the main results, discussed in Ref. [14], for a reciprocal asymmetric elementary cell, where the $\hat{C}$ axis of the right uniaxial layer is parallel to the x axis $(\alpha_R = 0)$, while the in-plane (x,y) $\hat{C}$ axis of the left layer is misaligned with an angle variation: $0 \leqslant \alpha_L \leqslant \pi/2$. Notice that the parameter values of our multilayer model were tailored [14] in order to accomplish the resonance condition between the photonic multilayer energy $\hbar\omega_r$ and the Wannier exciton transition energy $[E_{\rm ex}(0) = 1.418\,{\rm eV}]$ when the misalignment between the two optical axes is $\Delta\alpha = \alpha_L - \alpha_R = \pi/2$. First of all, let us consider a system with a spatially symmetrical elementary cell obtained for parallel orientation $(\Delta\alpha = 0)$ of the two optical axes. In this case the two linearly polarized waves (TE and TM) feel two different periodic dielectric values not in resonance with the chosen exciton energy [14]. Therefore, absolute gaps in the dispersion curves are highly unlikely, and many cross points between different polarization waves are present in the dispersion curves (see also Fig. 3 of Ref. [1]).

In Fig. 2(a) the dispersion curves are shown in a range of energy close to the unperturbed exciton energy. It is interesting to underline that the former behavior is not removed by the so-called exciton-polariton strong coupling; in fact, no polariton splitting is observed in the dispersion curves. This is due to the bulk symmetry of the system, which is a robust property; therefore, it can overcome the exciton-photon resonant interaction.

Now, for $\Delta\alpha \neq 0$, due to the collapse of the spatial symmetry, absolute gaps open, as fully discussed in Ref. [1]. In this case, for the whole range of the misalignment $(0 < \Delta\alpha < \pi/2)$ the x (TM polarization) and y (TE polarization) components of the electric field will be mixed by the out-of-diagonal elements of the in-plane dielectric tensor ε_L of Eq. (1a), and the optical response, computed for $\Delta\alpha \neq n\,\pi$, will be characterized by the simultaneous presence of the x and y amplitude components for both the TE and TM polarizations of the incident wave. In Fig. 2(b) the case of $\Delta\alpha = 10^\circ$ is shown, and two absolute gaps are present.

Two TE and TM linear polarized waves that propagate in an N cluster with misalignment have the same in-plane dielectric tensor sequence but with a different order. However, this difference does not affect the optical response [1,14]. This clearly appears in Figs. 3(a) and 3(b), where the transmission and reflection, computed for the two polarizations and for $\Delta\alpha = \pi/2$, in a cluster of $N = 32$ elementary cells are reported. The line shapes of the forward TM and TE incident-wave polarizations are exactly superimposed on one another

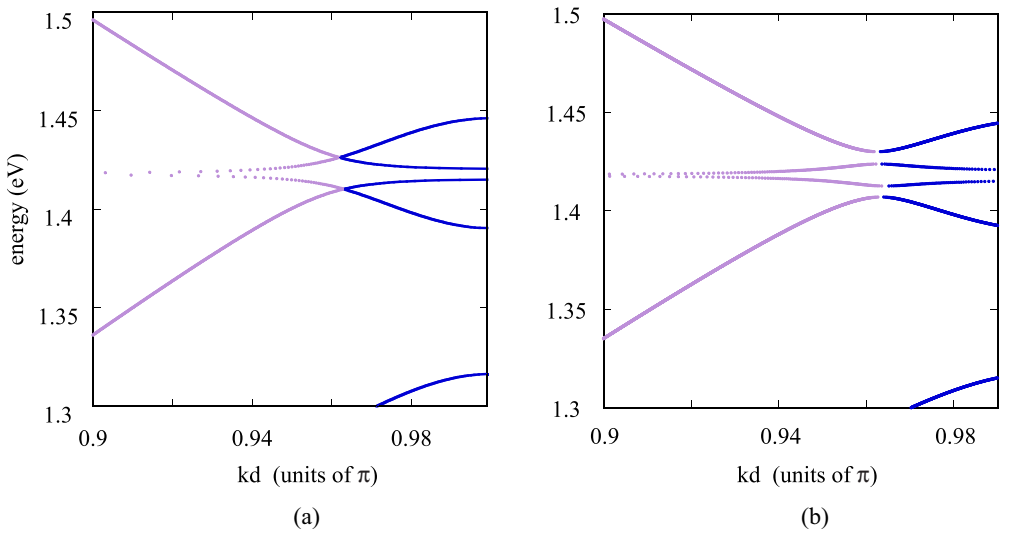

FIG. 2. Photon dispersion curves at normal incidence in the range of exciton-polariton energies. The x-polarized eigenvalues are represented by mauve dots, and the y-polarized ones are shown by blue dots. The x and y polarizations are used to indicate the majority contribution of the x or y component to the electric field intensity. (a) $\Delta\alpha = 0^\circ$ (no absolute gap is present). (b) $\Delta\alpha = 10^\circ$ (two absolute gaps are present).

in the whole photon energy range. But for energies rather close to the exciton-polariton resonance, where the intensity of the absorbance shows strong dependence on the polarization, the reflection and transmission shapes appear strongly deformed, and moreover, two giant transmission peaks are present at the optical band edges [14].

The above behavior can be highlighted, in a more general way, by the data in Fig. 4(a), where the computed absorbance intensities are reported as a function of the detuning between the exciton energy $E_{\rm ex}(0)$ and the resonance energy of the photonic crystals ($\hbar\omega_r = 1.414$ ev). Notice that, even for different energy values, we see the same trend for the TM and TE polarizations, but the intensity values strongly differ for energies close to the resonance.

Finally, Fig. 4(b) shows the FWHM of the absorbance computed as a function of the quantum well number N. Clearly, for N values greater than 30, the forward TM polarization saturates to its maximum value, while the TE polarization saturates to its minimum value. These behaviors allow us to underline how the optical response of a cluster of 32 cells is rather close to that of a $N \to \infty$ bulk [19].

Notice that in a uniaxial multilayer, we can mix TE and TM components not only with the incident wave with mixed polarization but also with the misalignment with $\Delta\alpha \neq n\,\pi$ ($n = 0,1,2,\ldots$) of the two in-plane optical axes. While the TE and TM contributions to the incident wave give a linear combination of the pure polarized spectra, the out-of-diagonal matrix elements of the dielectric tensor ε_L strongly influence the optical line shapes, and a rearrangement of the optical gaps as a function of the cluster dimension can be observed, as already discussed in Ref. [14].

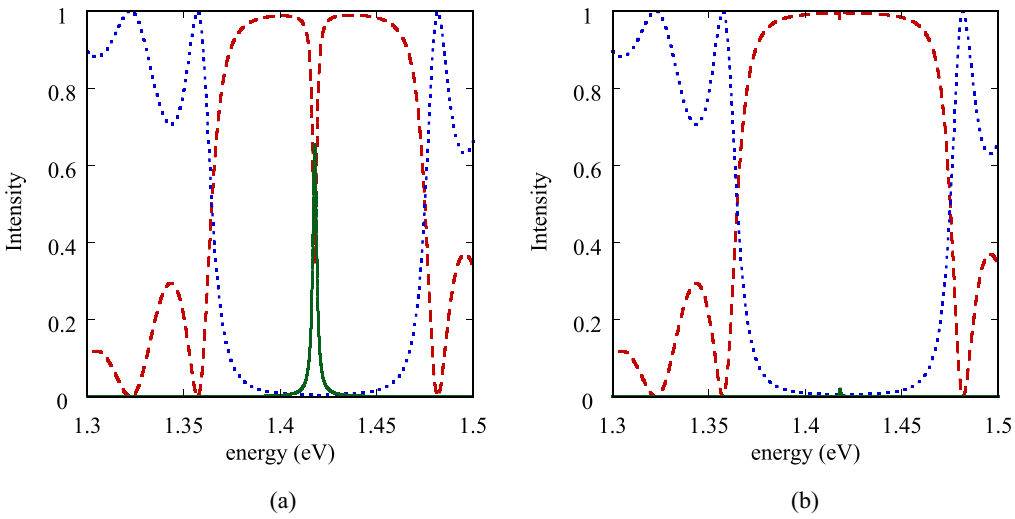

FIG. 3. Optical response at normal incidence. $\Delta\alpha = 90^\circ$. Reflectivity: dashed red line; transmission: dotted blue line; and absorbance: solid green line. (a) Forward incident waves are TM polarized, while backward ones are TE polarized. (b) Forward incident waves are TE polarized, while backward ones are TM polarized.

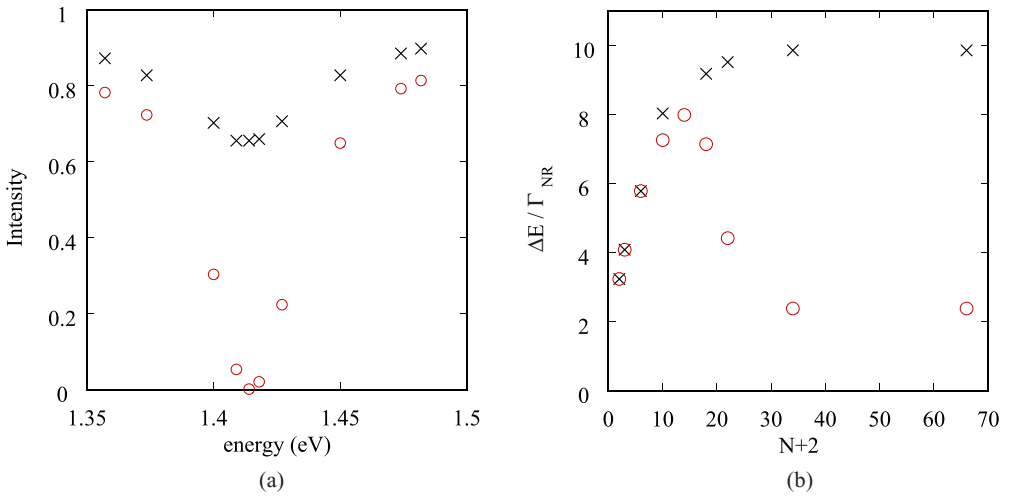

FIG. 4. (a) Absorbance intensity computed as a function of the energy for normal incident TM (crosses) and TE (open circles) polarizations. $N = 32$. (b) FWHM of the absorbance peak, computed for the TM (crosses) and TE (open circles) polarizations as a function of the quantum well number.

Let us consider a cell (see Fig. 1) with an optical in-plane misalignment of $\Delta\alpha = \pi/4$, for which equal contributions of TE and TM polarizations are expected. We use now an asymmetric choice of the dielectric constants ($\bar{\varepsilon} \neq \varepsilon_b$), namely, $\varepsilon_\parallel = 12.24$ and $\varepsilon_\perp = 2.24$, and an exciton energy [$E_{\rm ex}(0) = 1.4762$ eV] in resonance with the lowest-energy gap.

In Ref. [14] it was underlined that under the former conditions the lowest-energy photonic gap shows a nondirect transition at the border of the BZ, and this interesting behavior is shown in Fig. 5(a), while Fig. 5(b) shows the exciton-polariton behavior in an enlarged energy scale and very close to the unperturbed exciton energy. Notice that the behavior of the exciton-polariton splitting [see Fig. 5(b)] of the otherwise twofold-degenerate exciton-polariton dispersion curves can be fully explained along the lines of Ref. [14], and therefore, it will be not repeated here. Moreover, since the dispersion curves in Fig. 5(a) show a clear pattern of three stationary points in the bottom band at the boundary of the BZ, this system should be well suited to obtain giant transmission peaks at the optical band edges, as underlined in Refs. [3,4].

In Figs. 6(a) and 6(b) the forward optical response of a cluster with $N = 32$ elementary cells and optical misalignment $\Delta\alpha = \pi/4$ is reported for forward TM and TE incident-wave polarizations, respectively. In the present case the two transmission peaks at optical band edges are both present, but only that on the low-energy side of the spectrum shows rather high intensity (<80%). These results underline that the dispersion curve analysis is a necessary but not sufficient condition to obtain giant transmission peaks in a finite cluster. Finally, for a nonsymmetric choice of the dielectric constants but with $\bar{\varepsilon} = 13.24 > \varepsilon_b$ (for instance, $\varepsilon_\parallel = 18.24$ and $\varepsilon_\perp = 8.24$),

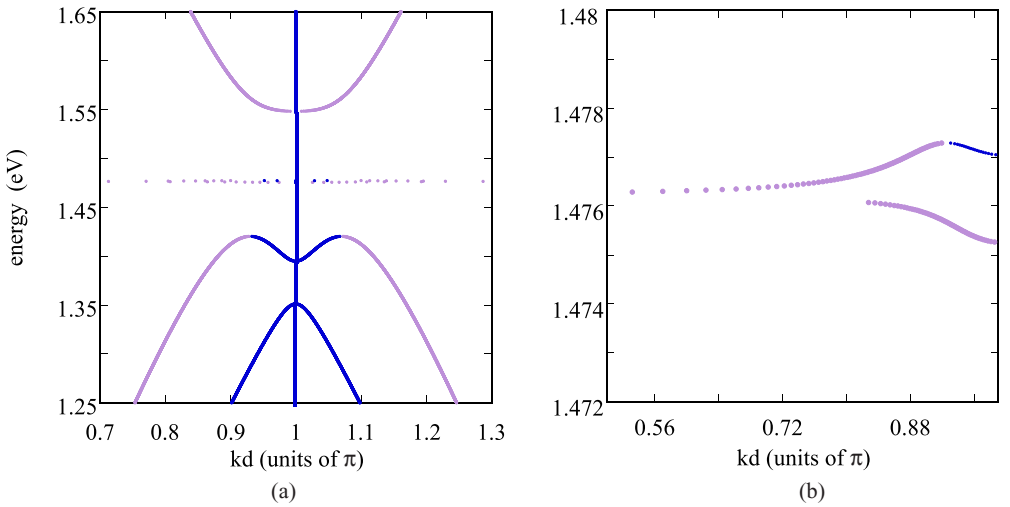

FIG. 5. The x-polarized eigenvalues are represented by mauve dots, and the y-polarized ones are shown by blue dots. The x and y polarizations are used to indicate the majority contribution of the x and y components to the electric field intensity, respectively. (a) Normal incidence dispersion curves of a reciprocal asymmetric elementary cell in the energy range of the first absolute gap. (b) Dispersion curves in an enlarged energy scale and close to the unperturbed exciton energy.

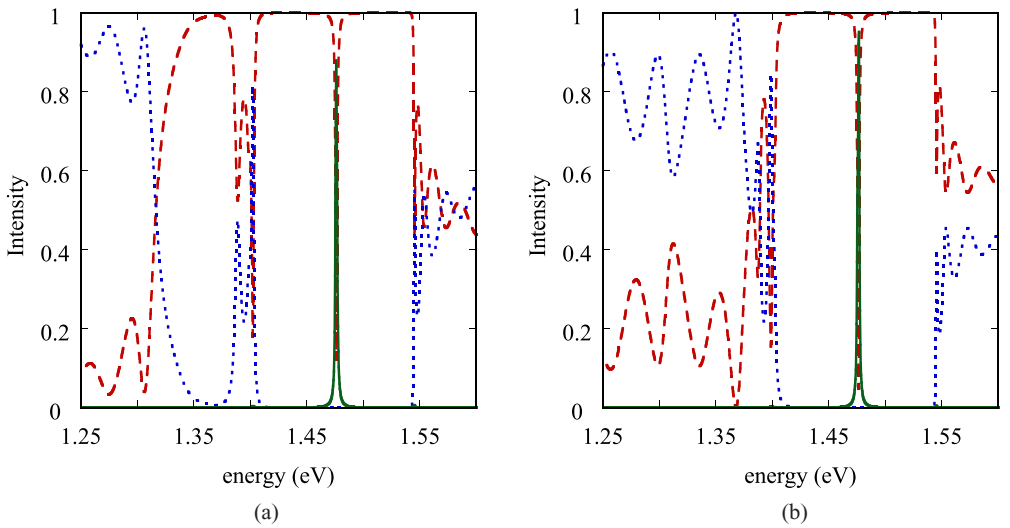

FIG. 6. Forward normal optical response of the reciprocal multilayer of Fig. 5(a). Reflectivity: dashed red line; transmission: dotted blue line; and absorbance: solid green line. (a) TM polarization. (b) TE polarization.

the optical upper and lower band behaviors are reversed, and the pattern of three stationary points appears in the upper optical band. In this case two high-intensity transmission peaks (not reported here) appear at both edges of the stop band, as discussed in Refs. [3,4].

IV. NONRECIPROCAL ELEMENTARY CELL

It is well known that nonreciprocal optical properties in a periodic multilayer can be obtained by removing spatial inversion and time-reversal symmetry by using magnetic materials or by imposing an external magnetic field. Therefore, in this case the dispersion curves could be $\hbar\omega(\mathbf{K}) \neq \hbar\omega(-\mathbf{K})$ (bulk spectral asymmetry [2]), where $\mathbf{K} \equiv (\mathbf{k}_\parallel, \mathbf{k})$. $\mathbf{k}$ is the z component of the Brillouin wave vector of the elementary cell. In our case we will have to restrict to the so-called axial spectral asymmetry [2], namely, $\hbar\omega(\mathbf{k}_\parallel, \mathbf{k}) \neq \hbar\omega(\mathbf{k}_\parallel, -\mathbf{k})$, with $k_\parallel \neq 0$. In order to obtain the former result we will follow the reasoning of Ref. [2] by removing from the system the invariance with respect to the twofold rotation 2_z, and this can be easily obtained by two added conditions in our minimal model in Fig. 1; namely, (i) the orientation of the optical axis of the dielectric tensor of the uniaxial right layer [Eq. (1b)] will have a nonzero component along the z axis, and (ii) the dispersion curves have to be computed for non-normal incident scattering ($k_\parallel \neq 0$).

Now, let us rotate the $\hat{C}$ axis of the right uniaxial layer by 30° ($\alpha_R = 30^\circ$) on the (x,z) plane in order to obtain a nonzero z component of the electric field together with a non-negligible x component; moreover, the calculations are performed for an angle of incidence $\theta = 20^\circ$ with respect to the z axis. Notice that in the present optical geometry the TE and TM polarized wave interaction is obtained with the in-plane optical axis misalignment, while the incident wave vector still remains on the (x,z) plane [2,14].

The main effects induced by the non-normal incidence condition on the exciton-polariton propagation are as follows: (i) The photon components have a longer path in the system that moves the Bragg photon energy towards higher-energy values (for instance, in the former model for an incident angle of $\theta = 20^\circ$, with respect to the z axis, the resonant photon energy increases from 1.414 to 1.525 eV). (ii) The exciton energy increases by the kinetic contribution of the center-of-mass motion [see Eq. (2)]. (iii) The Wannier exciton strongly couples with a photon with an equal in-plane wave vector in order to produce a polariton composite particle (strong-coupling effect [17]).

Let us consider again the former symmetric dielectric constant values ($\varepsilon_\parallel = 12.24$ and $\varepsilon_\perp = 8.24$); the dispersion

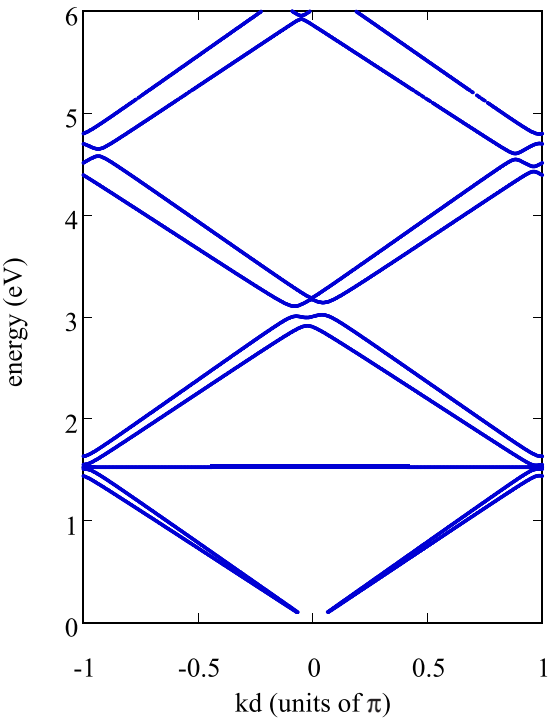

FIG. 7. Exciton-polariton dispersion curves of hybrid resonant photonic crystals with axial spectral asymmetry and dielectric functions: $\varepsilon_\parallel = 12.24$ and $\varepsilon_\perp = 8.24$. The exciton transition energy is $E_{ex}(0) = 1.525$ eV.

curves for a nonreciprocal hybrid multilayer are shown in Fig. 7. Notice that Wannier exciton energy is taken in resonance with the lowest absolute optical gap of the system [$E_{ex}(0) = 1.525$ eV]. The asymmetry for $\pm k$ values with respect to the Γ point is not evident in the scale of energy in Fig. 7. In fact, the gap at the left edge of the BZ ($k = -\pi/d$) is about $\Delta_L \approx 38$ meV, while at the right edge ($k = \pi/d$) it is $\Delta_R \approx 31$ meV; therefore, the width of the first absolute band gap is about 31 meV.

In order to study the degree of asymmetry of the dispersion curves let us consider the difference in energy between the left and right lowest-energy gaps, computed by the following sequence of symmetric dielectric functions: $\Delta\varepsilon = \varepsilon_{\parallel} - \varepsilon_{\perp} = 4n$, where $n = 1,2,3,4$. The energy differences $E_{gL} - E_{gR}$ are, respectively, $38 - 31 = 7$ meV, $62 - 39 = 23$ meV, $92 - 12 = 10$ meV, and $205 - 145 = 40$ meV; therefore, the absolute gap coincides with the right gap in these systems.

Figure 8(a) shows the dispersion curves for the last couple of dielectric constants ($\varepsilon_{\parallel} = 18.24$ and $\varepsilon_{\perp} = 2.24$) where the exciton transition energy is in resonance with the first absolute photonic gap [$E_{ex}(0) = \hbar\omega_r = 1.735$ eV]. Notice that for this rather large birefringence value ($\Delta\varepsilon = 16$) the dispersion curves show large asymmetry starting from the second absolute gap. Moreover, this new gap, which is very narrow in energy ($\sim$31 meV), drops well inside the negative k values of the BZ, while its shape is very close to the open gap due to a pair of Dirac points [11,16] in 2D systems [see also Fig. 9(a)]. In fact, Fig. 8(b) shows the dispersion curves of the non-normal symmetric case ($\theta = 20^\circ$ and $\alpha_L = \alpha_R = 0^\circ$), where two cross points, at a photon energy of about $\hbar\omega \approx 3.5$ eV and symmetric with respect to the Γ point ($kd = \pm 0.25$), are clearly reported.

Now, by rotating the optical axis on the (x,z) plane of $\alpha_R = 30^\circ$, the two cross points become asymmetric ($kd = -0.25$ and 0.0) with respect to the Γ point of the BZ (the picture is not reported here). Finally, by rotating the in-plane optical axis of $\alpha_L = 45^\circ$, the optical gaps open at the former cross-point energies, as shown in Fig. 8(a).

In conclusion, while the synergic effect of non-normal incidence ($\theta = 20^\circ$) and the orientation ($\alpha_R = 30^\circ$) of the optical axis on the (x,z) plane make the two cross points (located at about $\hbar\omega \approx 3.5$ eV photon energy) asymmetric, the orientation ($\alpha_L = 45^\circ$) of the optical axis on the (x,y) plane opens a new absolute gap close to the left cross point of the bands [14]. Notice that the last consideration justifies the adopted name "minimum model" and is the most interesting result of the present work.

In Fig. 9(a) the former small absolute gap is reported on an enlarged energy scale, and five stationary points, with zero group velocity, are present in the top and bottom photonic bands. Notice that a photon with energy in resonance with the inflection point of the bottom band ($\hbar\omega \approx 3.5175$ eV) crosses the band in two different points, namely, (i) a point close to the Γ point, where an inflection point with zero group velocity is observed, and (ii) a cross at $k < 0$, where the group velocity is negative; therefore, only the last wave can transfer electromagnetic energy, and a unidirectional propagation effect is obtained [2,16] in these nonmagnetic crystals.

Analogous considerations can be performed for photon energy in resonance with a minimum in the upper band ($\hbar\omega \approx 3.7905$ eV); in this case the former inflection point is now substituted by a minimum, and two crosses are observed in correspondence with negative values of k; therefore, the two group velocities have different signs, and no unidirectional propagation is present [6,16].

The former description is well suited for weak exciton-photon interaction, while in the presence of strong radiation-matter interaction a more complex behavior is present, as shown in Fig. 9(b), which, on a further enlarged energy scale, reports the polariton splitting for a Wannier exciton in resonance with the inflection point of the bottom band. Notice that the former inflection point in Fig. 9(a) now becomes a bunch of negative k values with zero group velocity, while the cross point at $k < 0$ is removed by polariton splitting, and a rather flat dispersion polariton curve, due to the strong radiation-matter interaction, is present very close

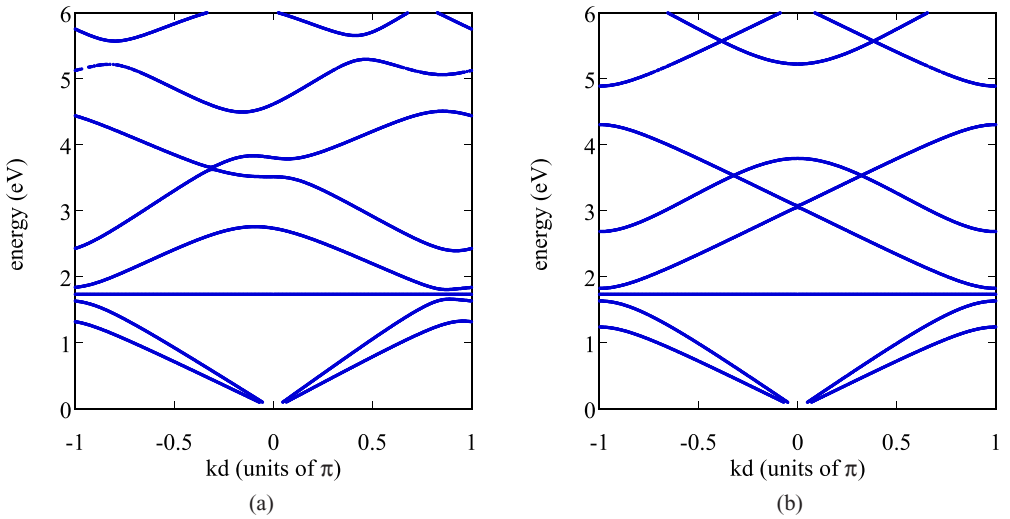

FIG. 8. Exciton-polariton dispersion curves of hybrid resonant photonic crystals. $E_{ex}(0) = 1.735$ eV, $\varepsilon_{\parallel} = 18.24$, $\varepsilon_{\perp} = 2.24$,$\theta = 20^\circ$. (a) Axial spectral asymmetry: $\alpha_L = 45^\circ$, $\alpha_R = 30^\circ$, $k_{\parallel} \neq 0$, $\varepsilon_{xz} \neq 0$. (b) Axial spectral symmetry: $\alpha_L = 45^\circ$, $\alpha_R = 0^\circ$, $k_{\parallel} \neq 0$, $\varepsilon_{xz} = 0$.

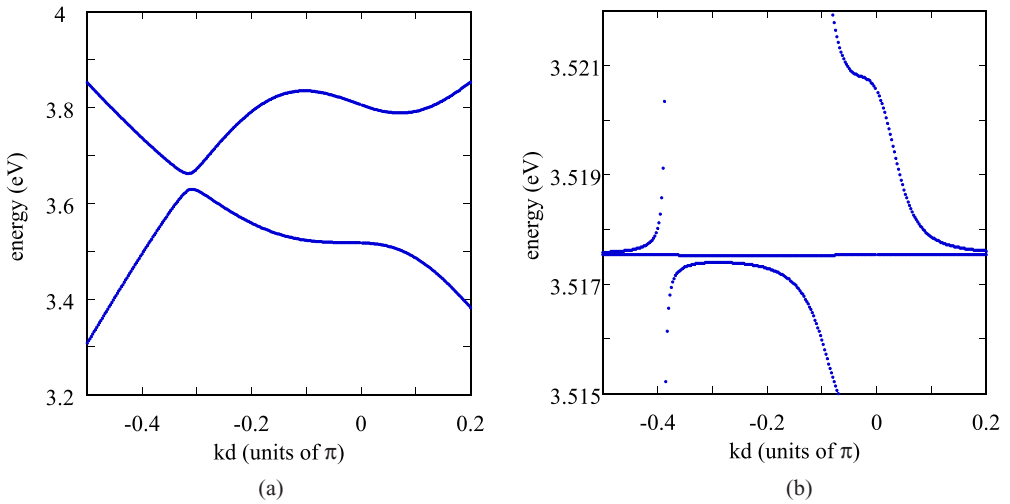

FIG. 9. Dispersion curves of Fig. 8(a) in enlarged energy scales: (a) close to the energy of the second absolute energy gap and (b) close to the exciton energy [$E_{ex}(0) = 3.5175$ eV] in resonance with the stationary inflection point.

to the unperturbed exciton energy [13,14] [calculated by Eq. (2) using $E_{ex}(0) = 3.5175$ eV]. Moreover, since in the present case, in which many symmetry operations have been removed, the coupling among upper and lower bands and the two so-called exciton-polariton intermediate bands is between the upper band and the lower intermediate band and the lower band and the upper intermediate band [see also Fig. 4(b)], the surprising presence in the dispersion curves of a rather unperturbed intermediate band with zero group velocity can be explained by the former interaction.

Finally, the nonreciprocal hybrid photonic crystal enlarges the zone of k values with zero group velocity a great deal, and this property is crucial for storing the light impulse on hybrid superstructures, as discussed in Ref. [14].

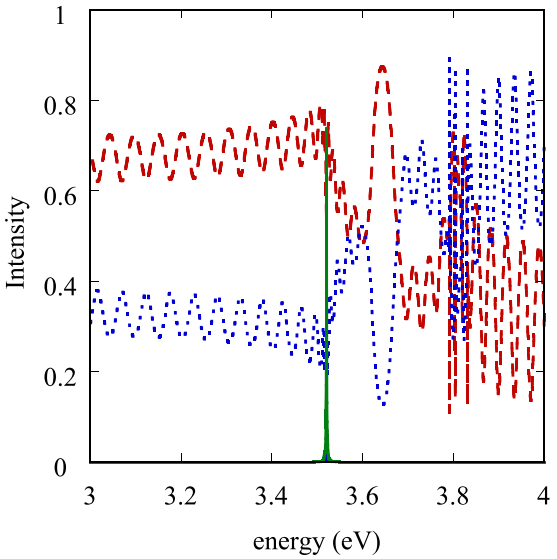

FIG. 10. Forward optical response for an S-polarized non-normal incident wave on a hybrid cluster of $N = 32 + 2$ quantum wells for the bulk parameter values in Fig. 9(b). Reflectivity: dashed red line; transmission: dotted blue line; and absorbance: solid green line.

Notice that in the present calculation, in order to accomplish resonant conditions and to observe the effect of strong radiation-matter interaction (polariton splitting), we have shifted the exciton energy $E_{ex}(0)$ in a rather large range of energies (from 1.418 to 3.6434 eV) while the other parameter values of the model remain unchanged. Obviously, the former exciton energy variation is outside the possibility of the quantum confinement in the AlGaAs/GaAs(001) system; therefore, our results should be considered a qualitative suggestion because rather different materials (for instance, gallium nitride [20] and semiconductor oxides [21]) with stronger radiation-matter interaction should be considered for observing unidirectional propagation in the strong-coupling regime in the second absolute gap of these nonmagnetic photonic crystals. Finally, the properties observed for uniaxial dielectric constant values ($\varepsilon_{\parallel} = 18.24$, $\varepsilon_{\perp} = 2.24$) can be obtained also for different uniaxial dielectric constant values, for instance, 15.24, 2.74; 12.24, 2.94; and 10.24, 3.24.

For the sake of completeness, the forward optical response for a TE polarized non-normal incident wave in a hybrid cluster of $N = 32 + 2$ quantum wells, computed for the same bulk parameter values as in Fig. 9(b), is reported in Fig. 10. It is interesting to note that the small absolute gap is just present in this cluster, while the exciton energy is in resonance with the inflection point of the bottom band ($\hbar\omega = 3.5175$ eV). Moreover, the five stationary points reported in Fig. 9(a) are in one-to-one correspondence with the strong change in the diffraction oscillations present in Fig. 10.

V. CONCLUSIONS

In conclusion, using selected numerical examples, we have discussed the no-absorption effect under resonant conditions and the presence of the transmission peaks at the optical band edges in periodic hybrid crystals with a spatially asymmetric elementary cell.

The optical nonreciprocity [$\hbar\omega(k_{\parallel},k) \neq \hbar\omega(k_{\parallel}, -k)$] is obtained by removing axial rotation 2_z and computing the dispersion curves in a semi-infinite periodic lattice for oblique

incidence ($\theta = 20^\circ$). The unidirectional properties are computed in such a structure for selected parameter values of the model; in particular, we have discussed the optical properties of a hybrid system with uniaxial dielectric constant values ($\varepsilon_\parallel = 18.24$, $\varepsilon_\perp = 2.24$). We should underline at this point that the above choice of parameter values is not restrictive in order to obtain unidirectional propagation of light when the cell possesses axial asymmetry.

The influence of strong radiation-matter coupling on the exciton-polariton propagation at non-normal incidence was studied in a high-quality sample [14] by computing nonreciprocal dispersion curves in the zone of exciton-photon resonance. Finally, the characteristic inflection points present in nonreciprocal dispersion curves were studied with a linear polarized optical response in a cluster of $N = 32$ asymmetric elementary cells.

[1] C. Vandenbem, J.-P. Vigneron, and J.-M. Vigoureux, J. Opt. Soc. Am. B **23**, 2366 (2006).

[2] A. Figotin and I. Vitebskiy, Phys. Rev. E **68**, 036609 (2003).

[3] A. Figotin and I. Vitebskiy, Phys. Rev. E **72**, 036619 (2005).

[4] A. Figotin and I. Vitebskiy, Phys. Rev. A **76**, 053839 (2007).

[5] A. Figotin and I. Vitebskiy, Phys. Rev. B **77**, 104421 (2008).

[6] A. Figotin and I. Vitebskiy, Phys. Rev. B **67**, 165210 (2003).

[7] A. Kavokin, G. Malpuech, and M. Glazov, Phys. Rev. Lett. **95**, 136601 (2005).

[8] J. J. Davies, D. Wolverson, V. P. Kochereshko, A. V. Platonov, R. T. Cox, J. Cibert, H. Mariette, C. Bodin, C. Gourgon, E. V. Ubyivovk, Y. P. Efimov, and S. A. Eliseev, Phys. Rev. Lett. **97**, 187403 (2006).

[9] E. Cancellieri, F. M. Marchetti, M. H. Szymanska, D. Sanvitto, and C. Tejedor, Phys. Rev. Lett. **108**, 065301 (2012).

[10] P. Bhattacharya, B. Xiao, A. Das, S. Bhowmick, and J. Heo, Phys. Rev. Lett. **110**, 206403 (2013).

[11] A. V. Poshakinskiy, A. N. Poddubny, L. Pilozzi, and E. L. Ivchenko, Phys. Rev. Lett. **112**, 107403 (2014).

[12] L. Pilozzi, A. D'Andrea, and K. Cho, Phys. Rev. B **76**, 245312 (2007).

[13] L. Pilozzi, A. D'Andrea, and K. Cho, Phys. Rev. B **69**, 205311 (2004); A. D'Andrea and D. Schiumarini, Eur. Phys. J. B **54**, 87 (2006).

[14] D. Schiumarini, A. D'Andrea, and N. Tomassini, J. Opt. **18**, 035101 (2016).

[15] Z. S. Yang, N. H. Kwong, R. Binder, and A. L. Smirl, J. Opt. Soc. Am. B **22**, 2144 (2005).

[16] F. D. M. Haldane and S. Raghu, Phys. Rev. Lett. **100**, 013904 (2008).

[17] K. Cho, *Optical Response of Nanostructures: Microscopic Nonlocal Theory* (Springer, Berlin, 2003); A. Stahl and I. Baslev, *Electrodynamics of the Semiconductor Band Edge*, Springer Tracts in Modern Physics Vol. 110 (Springer, Berlin, 1987).

[18] D. Schiumarini, N. Tomassini, L. Pilozzi, and A. D'Andrea, Phys. Rev. B **82**, 075303 (2010).

[19] We would like to underline that the two pictures in Figs. 4(a) and 4(b) and the related discussion are completely omitted in Ref. [14].

[20] C. Cobet, N. Esser, J. T. Zettler, W. Richter, P. Waltereit, O. Brandt, K. H. Ploog, S. Peters, N. V. Edwards, O. P. A. Lindquist, and M. Cardona, Phys. Rev. B **64**, 165203 (2001).

[21] P. Gori, M. Rakel, C. Cobet, W. Richter, N. Esser, A. Hoffmann, R. Del Sole, A. Cricenti, and O. Pulci, Phys. Rev. B **81**, 125207 (2010).